

Counter-intuitive properties of a simple quantum heat engine

Thiago R. de Oliveira* and Daniel Jonathan
*Instituto de Física, Universidade Federal Fluminense,
Av. Gal. Milton Tavares de Souza s/n, Gragoatá 24210-346, Niterói, RJ, Brazil*

We show that a quantum heat engine operating between two thermal baths may exhibit unusual responses to changes in the baths' temperatures. For example, its thermodynamic efficiency may increase as their temperature difference decreases. Conversely, the engine may cease to operate if the hotter bath becomes too hot, or the colder bath too cold, even in the limit of absolute zero temperature. Moreover, in some circumstances it may run in either sense of the same thermodynamic cycle, with the physical heat reservoirs exchanging the roles of 'hot' or 'cold' bath. In these cases there is a 'temperature gap': a finite range of temperatures for one of the baths within which no engine is possible, and on either side of which the engine runs in opposite senses. We demonstrate these and other counter-intuitive phenomena using a simple model of a quantum Otto cycle whose 'working substance' is a pair of spins coupled by the isotropic Heisenberg interaction. Quantum correlations play no role in these effects, which are due solely to the structure of the energy spectrum. We explain many of them, and also previously reported efficiency gains exhibited by this model, using a simple physical picture in terms of energy flows via each system level.

There has been a recent resurgence of interest in Quantum Thermodynamics [1], and in particular in microscopic engines operating in the quantum regime [2, 3]. A major goal is to understand how these quantum engines may differ from their classical counterparts. It is already known, for example, that energy-basis coherence may be used to boost engine efficiency [4, 5], a phenomenon that has recently been observed experimentally [6]. A closely related mechanism [8, 9] is to exploit ergotropy - energy extractable by unitary rotation, without changing a system's entropy [7]. Efficiency can also be boosted when at least one of the heat reservoirs interacting with the engine is not actually in thermal equilibrium [8–10], in particular when it is in fact a quantum measuring device [11, 12]. On the other hand, despite many attempts, no firm link has been found between efficiency gains and the presence of quantum correlations between subsystems of the 'working substance' [13–21].

In this article, we analyze a quantum engine, operating between two thermal baths, that exhibits efficiency gains without relying on any of these mechanisms. Rather, we explain them using a physical picture in terms of counter-propagating heat flows via different system levels. Moreover, we show that this model exhibits unusual *qualitative* responses to changes in the baths' temperatures. For example, the engine may become less efficient, or even stop working altogether, when the temperature gradient increases. It may also produce work while running in either sense of the same thermodynamic cycle (Fig. 1).

This engine's 'working substance' is a system of two spin-1/2 particles coupled via the Heisenberg interaction and placed in an external static magnetic field [22]:

$$H = 2J \vec{\sigma}_1 \cdot \vec{\sigma}_2 + h(\sigma_1^z + \sigma_2^z) - 2J \quad (1)$$

with $\vec{\sigma}_i = \{\sigma_i^x, \sigma_i^y, \sigma_i^z\}$ the Pauli matrices for site i , $J > 0$ the (antiferromagnetic) exchange coupling and $h > 0$ the

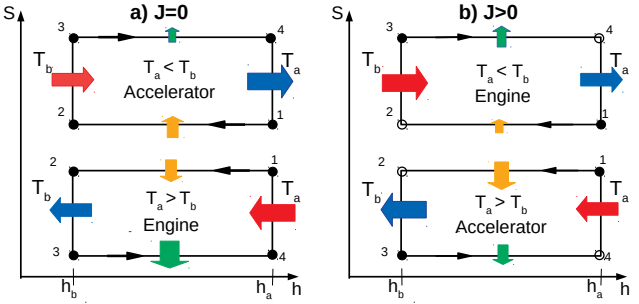


FIG. 1: (Color online) Otto cycles in an entropy (S) vs. field (h) diagram. Vertical (isochoric) strokes involve only heat exchange, represented by horizontal coloured arrows. Horizontal (adiabatic) strokes involve only work exchange, represented by vertical coloured arrows. Filled circles represent thermal equilibrium states. (a) With no coupling ($J = 0$), an engine must operate in an anti-clockwise cycle (bottom). A clockwise cycle (top) can represent either an accelerator (depicted) or a refrigerator (not depicted). (b) For coupled spins ($J > 0$) an engine may also operate clockwise, and an accelerator anti-clockwise. Other modes of operation are also possible in either cycle sense, see Fig. 2.

magnetic field [27]. The constant $-2J$ is added so that the eigenvalues of H have the simple forms $-8J$, $-2h$, 0 and $+2h$. The fact that only two of these depend on the field will prove particularly convenient below. For definiteness, we will refer to these energies as $E_{1,2,3,4}$, in this order, regardless of the relative magnitudes of J and h . Their respective eigenvectors are $\frac{1}{\sqrt{2}}(|\uparrow\downarrow\rangle - |\downarrow\uparrow\rangle)$, $|\downarrow\downarrow\rangle$, $\frac{1}{\sqrt{2}}(|\uparrow\downarrow\rangle + |\downarrow\uparrow\rangle)$ and $|\uparrow\uparrow\rangle$. The corresponding thermal state $\rho(h, J, T) = \frac{1}{Z} e^{-H/T}$ at temperature T is diagonal in this basis with elements $p_i \equiv \frac{e^{-E_i/T}}{Z}$, where $Z(h, J, T) = 1 + e^{8J/T} + 2 \cosh(\frac{2h}{T})$ is the partition function.

Otto Cycle – We subject this system to an Otto cycle consisting of two (quantum) adiabatic strokes and two isochoric strokes (Fig. 1). In the former, the system is

* troliveira@id.uff.br

isolated from external reservoirs while the magnetic field h is slowly varied between the limits h_b and $h_a > h_b$. The populations of each level remain constant - as does the von Neumann entropy S . In the latter, h is kept fixed and the system interacts with an external thermal reservoir until equilibrium is reached. We use T_a, T_b to denote the respective equilibrium temperatures at $h = h_{a,b}$, without specifying which is the hotter one. It is useful to define the ‘compression ratio’ $r = h_a/h_b > 1$.

Using standard definitions [2, 3], it is straightforward to calculate the average heat and work exchanges in this cycle [22]. During the isochoric strokes the Hamiltonian H is fixed, so only heat is exchanged: $Q = \text{Tr}[H(\rho_f - \rho_i)]$. During the adiabatic strokes only work is exchanged: $W = \text{Tr}[\rho(H_i - H_f)]$. For simplicity, we assume that no level crossings occur [28].

Regardless of whether the cycle is performed clockwise or anti-clockwise, the heat exchanged with the baths at temperatures $T_{a,b}$ can be written as

$$Q_a = -8J(p_1^a - p_1^b) + 2h_a(f_b - f_a) \quad (2)$$

$$Q_b = -8J(p_1^b - p_1^a) + 2h_b(f_a - f_b), \quad (3)$$

where, $p_1^a \equiv p_1(h_a, J, T_a)$ and

$$f_j(h, J, T) \equiv p_2^j - p_4^j = \frac{2 \sinh 2h_j/T_j}{1 + e^{8J/T_j} + 2 \cosh[2h_j/T_j]} \quad (4)$$

The work exchanges are

$$W_{b \rightarrow a} = 2(h_a - h_b)f_b > 0 \quad (5)$$

$$W_{a \rightarrow b} = -2(h_a - h_b)f_a < 0 \quad (6)$$

$$W_{cycle} = W_{b \rightarrow a} + W_{a \rightarrow b} = 2(h_a - h_b)(f_b - f_a) \quad (7)$$

Clearly $W_{cycle} = Q_a + Q_b$, as required by the First Law. The Second Law is also automatically satisfied, even though the quantum system may transit through non-equilibrium states, since at the end of each cycle it returns to its initial state, and since the external baths are described by ordinary equilibrium thermodynamics.

Despite this, and despite the simplicity of the above equations, we find that when the coupling $J \neq 0$ these cycles display a number of counter-intuitive properties.

Uncoupled spins – It is useful to first review what happens when $J = 0$ [23, 24]. In this case, the quantum cycle behaves much like the familiar classical ideal-gas Otto cycle [25]. To see this, note that the cycle produces positive work $W_{cycle} > 0$ (i.e., behaves as a heat engine) if and only if $f_b > f_a$. For $J = 0$, the function $f(h, J, T)$ reduces to $\sinh(2h/T)/(1 + \cosh(2h/T))$, which increases monotonically with h/T , so $f_b > f_a \iff T_a > rT_b$. The same condition also implies $Q_a > 0, Q_b < 0$, so this heat engine cycle must be performed anti-clockwise on the $S - h$ diagram [29]. The efficiency of this engine is $\eta_0 = \frac{W_{cycle}}{Q_a} = 1 - \frac{1}{r}$, which is analogous to that of the classical Otto engine. Since $T_a > rT_b$, η_0 is indeed lower than the Carnot limit.

If we decrease T_a so that $f_a > f_b$, then Q_a, Q_b, W_{cycle} all change sign, and the cycle becomes clockwise. Two

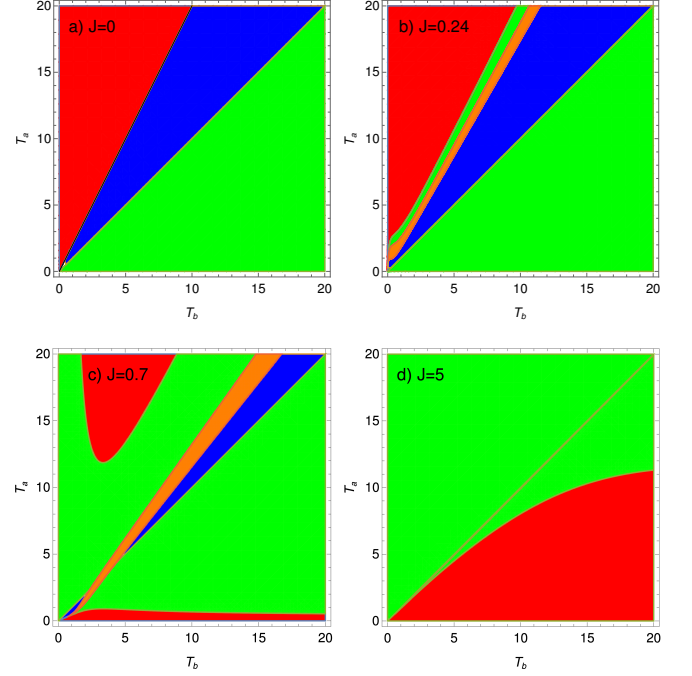


FIG. 2: (Color online) Ranges where the cycle operates as a refrigerator (blue/darkest), engine (red/darker), heater (orange/lighter), or accelerator (green/lightest) for different coupling strengths. The field values are $h_a = 2, h_b = 1$. All values of J, T, h are in the same (arbitrary) units [27]. Several remarkable phenomena can be inferred (see text).

other regimes of operation are then possible: for $T_b < T_a < rT_b$ we have a *refrigerator*, where heat flows out of the colder bath at T_b and into the hotter bath at T_a . When $T_a \leq T_b$ (Fig 1(a), top), we have an *accelerator*, where heat flows out of the hotter bath (now at T_b) and, at a higher rate, into the colder one. All these behaviors mirror closely those of the ideal-gas Otto cycle.

This correspondence can be attributed to the fact that, for uncoupled spins, the system remains throughout the cycle in an effective thermal state of the form $\rho(h, 0, T_{eff})$, so the quantum notion of an adiabatic evolution coincides with the thermodynamic one [23]. For example, during the $b \rightarrow a$ adiabatic stroke in Fig 1(a), the effective temperature T_{eff} increases continuously from T_b to rT_b , with $T_{eff}(h) = T_b \frac{h}{h_b}$ for $h_b \leq h \leq h_a$.

Coupled spins – When $J \neq 0$, however, no effective temperature can be defined during the adiabatic strokes, since the gaps between E_1 and the other levels shift at different rates [23]. In other words, in this case we have a non-equilibrium Otto cycle.

Let us now investigate the consequences. As a starting point, in Fig. 2 we plot, for different values of J , the ranges of temperatures T_a, T_b for which the cycle operates in each of the four possible regimes allowed by Thermodynamics. For $J = 0$, as previously discussed, only an engine (E), refrigerator (R) or accelerator (A) can occur, separated by the lines $T_a = rT_b$ and $T_a = T_b$.

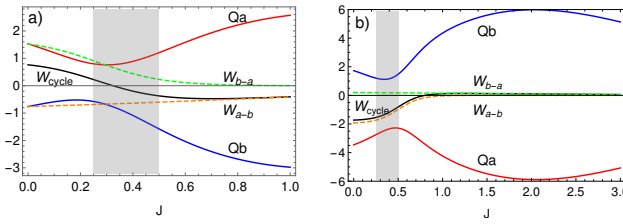


FIG. 3: (Color online) Work and heat as a function of the coupling J for $h_a = 2, h_b = 1$. (a) $T_a = 5, T_b = 1$. As J grows, the cycle transitions from an engine to an accelerator. (b) $T_a = 1, T_b = 10$. As J grows, the cycle transitions from an accelerator to a (very inefficient) engine. The shaded areas indicate the region $\frac{h_a}{4} < J < \frac{h_b}{4}$ where the machine cannot operate in the quantum adiabatic regime due to a level crossing [28], and our analysis does not apply.

As J increases, however, new features appear:

- (i) The original E - and R -zones shrink, while two new zones appear: a second A -zone, and also the previously forbidden *heater* (H), where $W_{cycle}, Q_a, Q_b < 0$ (work is converted into heat entering both baths).
- (ii) For sufficiently large J , a second E -zone also appears, within the region where $T_b > T_a$ (Fig. 2(c,d)). This remarkable phenomenon was noticed but not fully explored in Ref. [22]. It means that, unlike an ideal gas, this system can operate as an engine in *both* the clockwise and anti-clockwise senses of the cycle, as seen in Fig. 1.
- (iii) These two E -zones are separated by a *gap* in T_a , within which no heat engine is possible, regardless of T_b .
- (iv) Simultaneously, for *any* finite $T_a > T_b$, an engine becomes impossible as $T_b \rightarrow 0$. This is again remarkable - we usually expect that, the lower the cold bath temperature, the *easier* it is to run an engine;
- (v) Conversely, for $T_b > T_a$ an engine becomes impossible when T_b becomes too high - i.e., the hot bath can also become too hot. (Notice the downward slope of the lower E -zone in Fig. 2(c), for large enough T_b).
- (vi) Finally, for larger J , the H - and R -zones collapse to the line $T_a = T_b$ (Fig. 2(d)).

A qualitative mathematical understanding of these features can be obtained by noting that, due to the $e^{8J/T}$ term in Eq. (4), both $|W_{b \rightarrow a}|$ and $|W_{a \rightarrow b}|$ decrease rapidly with J , but at different rates. For $T_a > T_b$, the decrease in $|W_{b \rightarrow a}|$ is faster than that in $|W_{a \rightarrow b}|$. Consider a point inside the E -zone of Fig. 2(a), where $|W_{b \rightarrow a}| > |W_{a \rightarrow b}|$. As J grows, eventually this relation must invert, and W_{cycle} becomes < 0 by Eq. (7). By continuity, $Q_a > 0, Q_b < 0$ on both sides of the $W_{cycle} = 0$ border, so this point must in fact become an accelerator (thin green region in Fig 2(b)). This process is illustrated in Fig. 3(a). Other transitions, such as from refrigerator to heater to accelerator, can be similarly understood.

Conversely, for $T_b > T_a$ it is $|W_{a \rightarrow b}|$ that decreases faster as J grows. By an analogous argument, all points initially in the A -zone of Fig. 2(a) must eventually reach $W_{cycle} > 0$. This explains the appearance the new engine

zone. Furthermore, since initially $W_{cycle} < 0$ at all these points, this appearance requires J to be higher than a finite threshold. In Appendix A we show that the new E -zone cannot exist while $0 \leq J \leq h_b/4$, as in Fig. 2(a,b) but does for all $J > h_a/4$, as in Fig. 2(c,d). Since, as noted above, work exchanges fall exponentially with J , we can expect that engines operating in this regime will have a very small output (this can be seen in Fig. 3(b)).

Physically, the condition $J > h_a/4$ means that level $-8J$ remains the ground state throughout the cycle. In particular, in the limit $T_b \rightarrow 0$ it concentrates almost all the system's population after it thermalizes with bath b . But since it does not shift with the field h , the work $W_{b \rightarrow a}$ extracted in the expansion stroke becomes exponentially small. This is why, for any finite T_a , no engine is possible in this limit (property (iv) above). Analogously, we must always have an engine as $T_a \rightarrow 0$, for any finite T_b .

Property (iii) is then not too surprising: since an engine is impossible in the limit $T_b \rightarrow 0$, a single contiguous E -zone would necessarily cross the $T_a = T_b$ line. This would however violate the Second Law, for at the crossing point we would be extracting positive work from a single thermal reservoir.

In the Appendix we analyze Fig. 2 in greater mathematical detail. For example, in Appendix A2 are able to formally prove that a gap between the E -zones must indeed exist when $J > h_a/4$, and is in fact 'direct' (occurs at a specific value of T_b). In Appendix B we also derive asymptotic expressions for the inter-zone boundaries, which help to understand the shapes and disposition of the various zones. In particular, we explain properties (v) and (vi).

Physical Interpretation – A useful way to understand some of the features described above is by interpreting heat and work in terms of energy flows *via each level of the quantum system*. For instance: in eqs. (2),(3) the first term ($\equiv q_1^j$) is the heat exchanged with bath $j \in \{a, b\}$ via level 1, while the second term ($\equiv q_{24}^j$) represents heat exchanged via levels 2 and 4. In eqs. (5),(6) the work exchange is entirely via the latter, since only these levels shift with the field h .

Note now that, since q_{24}^a has the same sign as W_{cycle} , an engine cycle ($W_{cycle} > 0$) requires the net heat flux *via levels 2 and 4 only* to be directed from bath a - i.e., the one at a higher field value - to bath b , regardless of which of these is hotter. The reverse is true for refrigerator, accelerator or heater cycles. Meanwhile, since level 1 is not involved in work exchanges, all the heat it absorbs from one bath must be deposited in the other ($q_1^a = -q_1^b$).

It must be emphasized that the Second Law *does not apply* to these individual heat flows via specific levels; it only imposes constraints on the *overall* heat transfers after a full cycle. This allows some interesting combinations. Consider first the case $T_a > T_b$. In the engine regime, the heat flow via levels 2,4 is then indeed from the hot bath to the cold. However, the flux through level 1 may in principle occur *in either direction*, as long as the condition $Q_a > 0$ is respected (Fig. 4(a,b)).

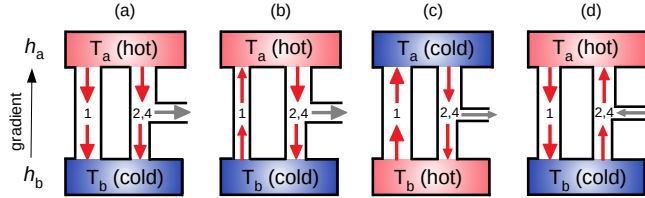


FIG. 4: (Color online) Energy transfer diagrams for various regimes of operation. The left and right channels represent respectively heat flowing via level 1 and via levels 2 and 4. (a) An ‘ordinary’ engine, i.e., one that functions as in the uncoupled case (Fig. 1(a)). (b) An engine that cycles in the ‘ordinary’ sense, but with enhanced efficiency $\eta > \eta_0$. (c) A ‘counter-rotating’ engine, (Fig. 1(b)). (d) A ‘counter-rotating’ accelerator, such as in Fig. 1(b). Regimes (b)-(d), which exhibit counter-propagating heat fluxes along the two channels, are only possible in the presence of coupling $J \neq 0$.

Reciprocally, when $W_{cycle} < 0$ we must have $q_{24}^a < 0$, so heat flows from the cold bath to the hot via these levels. In the case of an accelerator, for which $Q_a > 0$, this necessarily requires $q_1^a > -q_{24}^a > 0$; i.e., the flow via level 1 must be in the opposite sense (Fig. 4(d)). For a heater, $-q_{24}^a > q_1^a > q_{24}^b > 0$. A refrigerator may have q_1^a in either sense, like the engine in the previous example.

In the case $T_a < T_b$, in order to operate as a (‘counter-rotating’) engine, the cycle still needs $q_{24}^a > 0$, but now this means a flow of heat from the cold to the hot bath – opposite to the overall sense required by the Second Law. This is only possible if $q_1^a < 0$, (and moreover $|q_1^a| > q_{24}^a$) (Fig 4(c)). Similarly, a refrigerator can only operate in this regime if $q_{24}^a < 0$ and $q_1^a > -q_{24}^a > 0$, and a heater again requires $-q_{24}^a > q_1^a > q_{24}^b > 0$. In this case it is accelerators than can operate with q_1^a in either sense.

Efficiency – As noted above, much of the study of quantum heat engines has focused on regimes where they outperform their classical counterparts. For this particular model, Thomas et al [22] have found that, in the case where $T_a > T_b$, the engine efficiency η satisfies

$$\frac{\eta}{\eta_0} = 1 - \frac{8J}{Q_a} (p_1^b - p_1^a). \quad (8)$$

Thus, if $p_1^b < p_1^a$, coupling allows the engine to achieve an efficiency higher than η_0 .

We can give this condition a simple interpretation in terms of the concepts from the last section. The quantity $8J(p_1^b - p_1^a)$ is precisely the heat flux q_1^a from bath a to bath b through level 1. If $p_1^a > p_1^b$, this flux is negative, (from b to a), even though an engine cycle with $T_a > T_b$ requires a net heat flux from a to b ! Enhanced efficiency occurs precisely when the heat flux through this level occurs in the opposite sense to the one dictated by the Second Law (Fig 4(b)). This makes sense: any heat flux from a to b via level 1 is wasted, as this level does not contribute to the work exchanges. For a given fixed Q_a , reversing this flux allows more heat to flow via levels 2, 4, boosting the conversion to work and hence the efficiency.

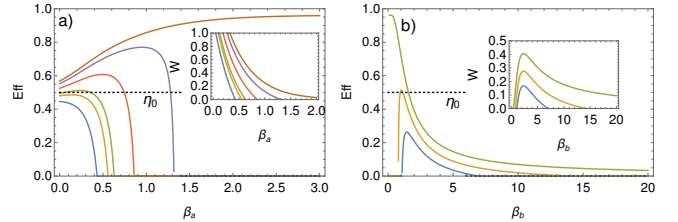


FIG. 5: (Color online) Efficiency η for fixed $J = 0.24$, $h_b = 1$, $h_a = 2$, and various temperature combinations. (a) η vs. $\beta_a \equiv T_a^{-1}$ for $T_b = 0.2, 0.1, 0.08, 0.05, 0.03, 0.001$ (from lower to upper curves). For $\beta_a \rightarrow 0$, η surpasses the uncoupled efficiency η_0 if T_b is under the threshold value $\frac{2h_b(h_b-4J)}{\ln 3} = 0.073$ [30]. It increases even further with β_a (i.e., as the temperature difference between the baths decreases). However, the work output W_{cycle} becomes exponentially small (inset). (b) η vs. $\beta_b \equiv T_b^{-1}$ for $T_a = 0.04, 0.03, 0.003$ (from lower to upper curves). In this case $\eta > \eta_0$ is achievable with finite work output (inset).

Another counter-intuitive phenomenon involving the efficiency is illustrated in Fig. 5. In Fig. 5(a) we plot η as a function of $\beta_a \equiv T_a^{-1}$, for various fixed values of T_b and a fixed $J \lesssim \frac{h_b}{4}$. Note first that, as $\beta_a \rightarrow 0$, η tends to a value above η_0 (dashed line) only when T_b is under a certain threshold. Moreover, in these cases the efficiency *increases further with β_a* (ie, as T_a decreases) [30]. This behaviour is contrary to the customary wisdom that a heat engine should become *less* efficient as one decreases the temperature gradient across which it operates. Physically what happens is that, as T_a falls, both the overall absorbed heat Q_a and the counter-propagating heat flux through level 1 reduce in magnitude, however the latter does so at a slower rate. By Eq. (8), this increases the efficiency. However, in this regime the extracted work W_{cycle} also falls to 0 exponentially with β_a .

A similar effect happens in the counter-rotating engine regime when $T_a \ll T_b$. In this case, as was previously mentioned, for any fixed T_a there is a finite T_b above which no engine is possible. It follows that, as $\beta_b \equiv T_b^{-1}$ is increased from zero, η will at a certain point change from zero to positive and continue to increase, at least for a while. This is shown in Fig. 5(b). In this case, however, W_{cycle} can remain finite for $\eta > \eta_0$ (see inset).

Discussion – We have shown that a simple quantum coupled-spin system can exhibit unusual thermodynamical properties when subjected to a nonequilibrium Otto cycle between two thermal baths. It can operate as an engine in either sense of the cycle, and in both cases may reach efficiency values beyond what is possible without coupling. In some circumstances, engine efficiency may increase when the temperature difference between the baths is decreased. Conversely, an engine can cease to be possible if the hot bath becomes too hot, or the cold bath too cold, or if the temperature of the bath at high magnetic field falls within a specific gap.

We have interpreted what happens in terms of separate heat transfers from one bath to another via each system level, showing that some of the effects occur when at least

one of these fluxes is in a direction contrary to that of the overall heat flow. We expect similar behaviours in other quantum models whose energy levels can be likewise split into those that depend on a given external parameter and those that do not - in particular when one of the latter is the ground state. It is an open question whether the same effects may also occur in models lacking this simple division, and if so how to interpret them.

It is worth emphasising that, unlike in Refs. [4–6, 8, 9], no energy-basis coherence or ergotropy have been exploited here - the system remains at all times in a passive, [7] energy-diagonal state. Moreover, our analysis relied exclusively on the system’s energy structure - all results would hold for a model with e.g. the same energies but whose eigenvectors were all product states - in which case the two spins would remain unentangled throughout the cycle. It can in fact be shown [26] that they also hold for a three-level (qutrit) model with energies $-8J, \pm 2h$. This proves that the presence of entanglement is not a necessary condition for the efficiency gains, confirming indications by previous studies [13–21].

Finally, it is not entirely clear whether the quantum nature of the model is a necessary condition for its unusual qualitative behaviours, or if they are rather an effect of the non-thermal intermediate states during the cycle. In particular, even though a discrete level structure seems to play a defining role in many of our arguments, we could not find a definite reason why those same behaviours might not be possible in a classical system, although we conjecture this is not the case. In any case, we were unable to locate any description of similar phenomena occurring in classical models.

ACKNOWLEDGMENTS

This work is supported by the Brazilian National Institute for Science and Technology of Quantum Information (INCT-IQ), and by the Air Force Office of Scientific Research under award number FA9550-19-1-0361.

Appendix A: General results

In this Appendix, we give more detailed statements and proofs of some results mentioned in the main text. Result 1 presents conditions for a ‘counter-rotating’ engine to be possible. Result 2 proves the existence of a ‘temperature gap’ for engine operation.

1. Conditions for engines with $T_b > T_a$

As noted above, one of the remarkable features of this coupled spin system is that it is able to operate as a heat engine in either sense (clockwise or anti-clockwise) of the Otto cycle, as depicted in an $S - T$ diagram. However, while a ‘normal’, anti-clockwise engine cycle (run-

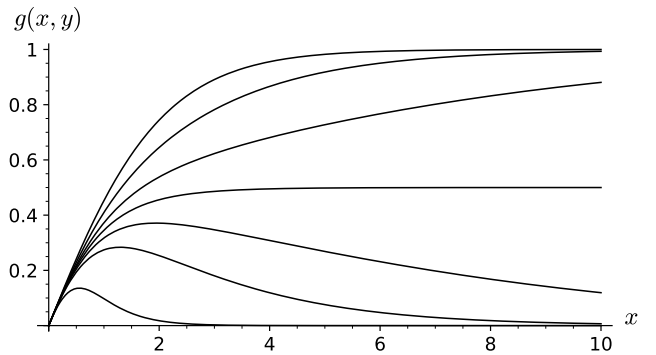


FIG. 6: Work function in the generic form $g(x, y)$ of Eq. (A3), shown as a function of x for various fixed values of y . From top to bottom: $y = 0.1, 0.5, 0.8, 1, 1.2, 1.5, 3$. For $y < 1$, the function increases monotonically towards 1 as $x \rightarrow \infty$. For $y = 1$, it tends asymptotically to 1/2. For $y > 1$, $g(x, y)$ is single-peaked and tends to 0 as $x \rightarrow \infty$.

ning with $T_a > T_b$) can exist for any value $J \geq 0$ of the coupling constant, a clockwise cycle (running with $T_b > T_a$) can only operate as an engine if the coupling is sufficiently strong. More specifically:

Result 1: Suppose $T_b > T_a$. (i) A cycle producing positive work $W_{cycle} > 0$ is impossible if $0 \leq J \leq h_b/4$. (ii) Conversely, if $J > h_a/4$, a cycle with $W_{cycle} > 0$ is possible for all T_b and sufficiently small T_a .

This result is illustrated in the fact that there is no red (E) zone in the bottom right half of Figs. 2(a,b), but one does appear in Figs. 2(c,d). Moreover, this bottom E-zone runs along the entire T_b -axis.

Proof of Result 1: As shown in Eqs. (4) - (6), the amount of work exchanged in each adiabatic stroke is proportional to the ‘work function’

$$f_j(h, J, T) = \frac{2 \sinh(2h_j/T_j)}{1 + 2 \cosh(2h_j/T_j) + e^{8J/T_j}}, \quad (A1)$$

where $j \in \{a, b\}$ denotes the starting point of the stroke. It is useful to rewrite this in the form

$$f_j(h, J, T) = g\left(\frac{2h_j}{T_j}, \frac{4J}{h_j}\right), \quad (A2)$$

where

$$g(x, y) = \frac{e^x - e^{-x}}{1 + e^x + e^{-x} + e^{xy}}. \quad (A3)$$

This function, shown in Fig. 6, has the following easily

checked properties for $x, y \geq 0$:

$$g(x, y) \geq 0; \quad g(x, y) = 0 \iff x = 0 \quad (\text{A4})$$

$$\lim_{x \rightarrow \infty} g(x, y) = \begin{cases} 0, & y > 1; \\ 1/2, & y = 1; \\ 1, & 0 \leq y < 1. \end{cases} \quad (\text{A5})$$

$$\frac{\partial g(x, y)}{\partial x} > 0 \text{ for } 0 \leq y \leq 1. \quad (\text{A6})$$

$$\frac{\partial g(x, y)}{\partial x} = 0 \text{ at a single value of } x, \text{ for } y > 1 \quad (\text{A7})$$

$$\frac{\partial g(x, y)}{\partial y} < 0. \quad (\text{A8})$$

$$g(rx, y) > g(x, ry) \text{ for } r > 1. \quad (\text{A9})$$

Suppose then that $T_b > T_a$, and $0 \leq J \leq \frac{h_b}{4}$, i.e., $J = s \frac{h_a}{4}$, for some $0 \leq s \leq 1$. In this case,

$$f_b - f_a = g\left(\frac{2h_b}{T_b}, s\right) - g\left(\frac{2h_a}{T_a}, \frac{s}{r}\right) < 0. \quad (\text{A10})$$

where we used Eq. (A9) and the fact that $r = \frac{h_a}{h_b} > 1$. [31]

By Eq. (7), this means $W_{cycle} < 0$, so no engine is possible for J in this range.

On the other hand, suppose $J = s \frac{h_a}{4}$, for some $s > 1$. In this case

$$f_b - f_a = g\left(\frac{2h_b}{T_b}, rs\right) - g\left(\frac{2h_a}{T_a}, s\right). \quad (\text{A11})$$

By Eq. (A5), $\lim_{T_a \rightarrow 0} f_a = 0$. Thus, for any fixed T_b we must have $f_b - f_a > 0 \Leftrightarrow W_{cycle} > 0$ when T_a is sufficiently small \square

2. Temperature gap

Another striking feature of this model, visible in Fig. 2(c), is the appearance of a *temperature gap* for T_a , that is, a range of values $T_a \in (T_{a1}, T_{a2})$ for which the cycle cannot operate at all as an engine - whatever the value of T_b . For T_a within this range, the work extracted during the expansion stroke of the cycle is always less than the one invested in the compression stroke.

We will now prove that such a gap always exists if the coupling J is sufficiently high. In fact, borrowing the terminology of solid-state physics, it is always a ‘direct gap’, in the sense that these two extremes of the gap range occur for the same value of T_b . Graphically, the lowest point of the ‘upper E-zone’ is always directly above the highest point of the ‘lower E-zone’.

Result 2: For $J > h_a/4$, there exists a range (T_{a1}, T_{a2}) of values of T_a for which $W_{cycle} < 0$, for any value of T_b . Furthermore: given h_a, h_b, J , there exists a temperature T_{b0} such that

(i) T_{b0} is the value of T_b that maximizes the work $W_{b \rightarrow a}$ extracted during the expansion stroke,

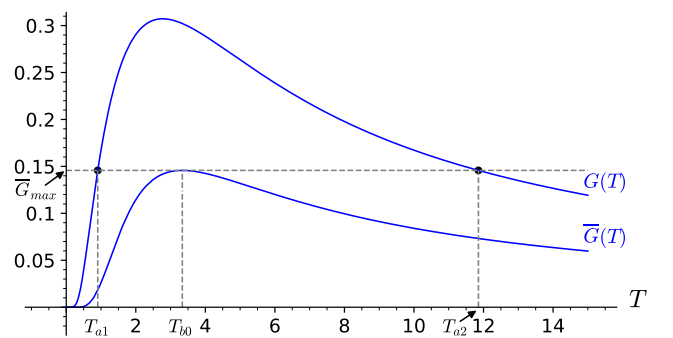


FIG. 7: Functions $G(T)$ and $\bar{G}(T)$ defined in Eq. (A13). The highlighted dots show the two points where $G(T)$ reaches the maximum value \bar{G}_{\max} of $\bar{G}(T)$. The interval $T_{a1} < T < T_{a2}$ where $G(T) > \bar{G}_{\max}$ corresponds to the gap in T_a where no engine can exist in Fig. 2(c). The temperature T_{b0} which maximizes $\bar{G}(T)$ is the point in T_b where the gap occurs. The parameters $h_a = 2$, $h_b = 1$, $J = 0.7$ are the same here as in that figure. For these values, $T_{a1} = 0.91$, $T_{b0} = 3.34$, $T_{a2} = 11.85$.

- (ii) $T_{b0} \in (T_{a1}, T_{a2})$, and
- (iii) $W_{cycle}(T_a, T_b) = 0$ for $(T_a, T_b) = (T_{a2}, T_{b0})$ and $(T_a, T_b) = (T_{a1}, T_{b0})$. In other words, the gap in T_a is ‘direct’ and occurs at $T_b = T_{b0}$

Proof of Result 2: We will base our analysis purely on the general mathematical properties (A4)-(A9) of $g(x, y)$. Note first that the borders of the E -zones are defined by the condition $W_{cycle} = 0$. For the case $J > h_a/4$, Eq. (A11) shows this condition is equivalent to

$$g\left(\frac{2h_a}{T_a}, s\right) = g\left(\frac{2h_b}{T_b}, rs\right) \quad (\text{A12})$$

where $r, s > 1$. Since we are assuming fixed h_a, h_b, J here, it is helpful to consider each side of this equation as a function only of T , e.g., to redefine

$$g\left(\frac{2h_a}{T_a}, s\right) \equiv G(T_a); \quad g\left(\frac{2h_b}{T_b}, rs\right) \equiv \bar{G}(T_b). \quad (\text{A13})$$

Let us now analyze the temperature ranges for which Eq. (A12) may or may not have solutions. Since $r, s > 1$, Eqs. (A4), (A5), (A7) imply that $G(T)$ and $\bar{G}(T)$ are single-peaked in T , and tend to 0 for $T \rightarrow 0, \infty$ (see Fig. 7 above). Let T_{b0} be the temperature where $\bar{G}(T_{b0})$ achieves its peak $\bar{G}_{\max} \equiv \max_T \bar{G}(T)$. Comparing the definitions of \bar{G} in Eq. (A13) and $W_{b \rightarrow a}$ in Eq. (5), using also Eq. (A2), we see this is the same as property (i).

Now: Eq. (A8) implies that

$$\bar{G}_{\max} = g\left(\frac{2h_b}{T_{b0}}, rs\right) < g\left(\frac{2h_b}{T_{b0}}, s\right) = G(rT_{b0}) \leq G_{\max} \quad (\text{A14})$$

where $G_{\max} \equiv \max_T G(T)$. Since $G(T)$ is single-peaked, it follows that, given any $T_b > 0$, Eq. (A12) will always be satisfied for exactly two values of T_a , that we will call $T_{a+}(T_b) > T_{a-}(T_b)$. (These solutions describe the upper and lower E -zone borderlines in Fig. 2(c)). In particular, if we define

$$T_{a1} \equiv T_{a-}(T_{b0}); \quad T_{a2} \equiv T_{a+}(T_{b0}),$$

then $G(T_{a1,2}) = \bar{G}_{\max} < G_{\max}$. Since $G(T)$ is single-peaked, $G(T_a) > \bar{G}_{\max} \iff T_a \in (T_{a1}, T_{a2})$. But this implies there is no solution for Eq. (A12) for T_a in this interval. More specifically, within this gap

$$W_{cycle} \propto (\bar{G}(T_b) - G(T_a)) < (\bar{G}_{\max} - G(T_a)) < 0, \quad \forall T_b.$$

Conversely, for any $T_a > T_{a2}$ or $< T_{a1}$, an analogous argument shows there will be two values of T_b that solve Eq. (A12). However, since \bar{G} is single-peaked, for $T_a = T_{a2}$ or $T_a = T_{a1}$ the only solution is $T_b = T_{b0}$. Thus we obtain property (iii).

We still need to prove property (ii). For the upper bound: by Eq. (A14), $G(rT_{b0}) > G(T_{a2}) = G(T_{a1})$. Since G is single-peaked, and by definition $T_{a2} > T_{a1}$, this implies $T_{a2} > rT_{b0} > T_{b0}$.

For the lower bound: Eq. (A9) implies that, in fact,

$$G(T) > \bar{G}(T), \quad \forall T > 0.$$

as can be seen in Fig. 7. But then $G(T_{b0}) > \bar{G}(T_{b0}) = G(T_{a1}) = G(T_{a2})$. Since G is single-peaked, this means that $T_{a1} < T_{b0} < T_{a2}$. Note that we reobtain also the upper bound in this way. However, as seen above, the latter is independent of property (A9) \square

In conclusion: the temperature gap in T_a appears due to the fact that, for large enough coupling J , the work function $f(h, J, T)$ becomes single-peaked in h/T . Physically, this occurs because, for large J , the ground state of this model becomes the level $-8J$, which does not contribute to the work exchanges in the adiabatic strokes, but which contains more and more of the system's population as $T \rightarrow 0$. The appearance of this gap can therefore be argued to be a quantum effect, since such a population accumulation in a single discrete state does not happen in classical systems.

It is worth emphasizing that, in the demonstration of Result 2, we only made use of properties (A4)-(A9) of the work function, and not of the specific form of $f(h, J, T)$. Since these are quite generic, we can expect that other, more complex models with similar characteristics will also exhibit a temperature gap where no engine operation is possible. An interesting open problem is to investigate more carefully to what extent properties such as Eqs. (A4)-(A9) are mandated by general constraints such as the Second Law, irrespective of the details of the Hamiltonian.[32]

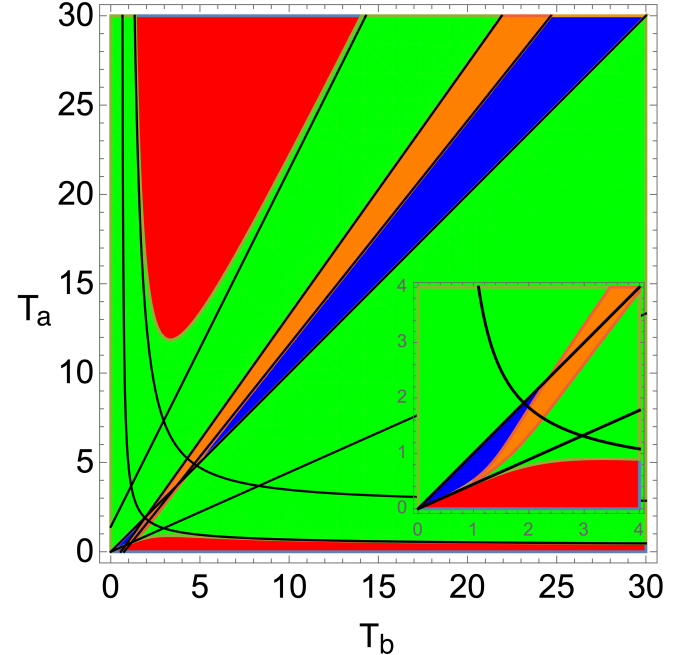


FIG. 8: (Color online) Asymptotic approximations for the borders of the various operation zones of the system. The system parameters are $h_a = 2$, $h_b = 1$, $J = 0.7$ (same as in Fig. 2(c)). As before, the the refrigerator (R) zones are in blue/darkest, the engine (E) zones in red/darker, the accelerator (A) in green/lightest, and the heater (H) in orange/lighter. The black lines are our asymptotic approximations to the various inter-zone boundaries. For the upper E -zone, these are given by Eq. (B7) (left side) and Eq. (B5) (right side). For the lower E -zone, they are given by Eq. (B9) (left side) and Eq. (B11) (right side). For the $A-H$, $H-R$ and $R-A$ borders, they are given respectively by Eqs. (B15), (B16) and (B21). The inset shows a closer view of the bottom left corner, omitting Eqs. (B15) and (B16) for clarity. Note in particular the second R -zone, corresponding to a 'counter-rotating' refrigerator ($T_b > T_a$)

Appendix B: Asymptotic Analysis

In this appendix we obtain simple asymptotic expressions for the borders of the various regions appearing in Fig. 2, allowing a greater understanding of their features.

These expressions also allow us to obtain Result 3, that shows that it is possible for the engine efficiency to increase even as the temperature gradient across which it operates decreases.

In this section we study how the system behaves when the temperatures T_a, T_b , become relatively 'large' or 'small' in comparison to each other or to other parameters. We use the resulting asymptotic formulae to understand the boundaries between the various zones appearing in the diagrams of Fig. 2 (see Fig. 8 above). Another application is to study the asymptotic behaviour of the heat engine efficiency η in the limit of large T_a . In particular, we demonstrate that η can increase as T_a decreases, for fixed T_b .

Our analysis is based on the following simple approximations:

- For ‘large’ temperatures, satisfying $2h_j/T_j \sim 8J/T_j \sim \varepsilon \ll 1$, we can express the work function in Eq. (A1), and more generally the probabilities p_1^j , as power series in ε :

$$f_j(h, J, T) = \frac{h_j}{T_j} - \frac{2h_j J}{T_j^2} + O(\varepsilon^3) \quad (\text{B1})$$

$$p_1^j = \frac{1}{4} \left[1 + \frac{6J}{T_j} + \frac{12J^2 - h_j^2}{T_j^2} \right] + O(\varepsilon^3) \quad (\text{B2})$$

- For ‘small’ temperatures $T_j \ll 8J, 2h_j$, the appropriate approximations are

$$f_j(h, J, T) \simeq \frac{1}{1 + \exp\left(\frac{8J - 2h_j}{T_j}\right)} \quad (\text{B3})$$

$$p_1^j(h, J, T) \simeq \frac{1}{1 + \exp\left(\frac{2h_j - 8J}{T_j}\right)}. \quad (\text{B4})$$

In other words, in this limit these functions behave as (complementary) step functions in J , with a sharp cutoff for $J > h_j/4$.

1. Asymptotic Zone Boundaries

Our first application is to obtain asymptotic expressions for the boundaries between the various operation regimes of the system. Figure 8 above illustrates the result of these calculations, which are detailed below. The figure is an expanded version of Fig. 2(c), with added lines corresponding to our asymptotes. We can see that agreement with the exact zone boundaries is generally extremely good, even for temperatures well within the depicted range.

a. Boundary of the upper E-zone

The boundaries of the E -zones are defined by the condition $W_{\text{cycle}} = 0$, which is equivalent to $f_a = f_b$ by Eq. (7). For the ‘upper’ ($T_a > T_b$) E -zone, we can solve this equation for T_a in the limits where (i) T_a and T_b are both ‘large’, or (ii) T_a is ‘large’ and T_b is ‘small’.

(i) Suppose $T_a \gtrsim T_b \gg 2J, 2h_a, 2h_b$. In this case it is possible to find T_a by an iterative (perturbative) method. Using Eq. (B1), we solve the equation $f_a = f_b$ to $O(\varepsilon)$, then substitute the solution into the equation to $O(\varepsilon^2)$, and so forth.

In this manner, it is possible in principle to obtain a complete series expression for the boundary line, valid in the limit of large T_b . The solution correct up to $O(\varepsilon)$, which is sufficient for our purposes, is

$$T_a = rT_b + 2J(r - 1) \quad (\text{B5})$$

Note that when $J = 0$ (no coupling), we recover asymptotically the exact E -zone boundary (Fig. 2(a)). For $J > 0$, Eq. (B5) shows that the boundary remains asymptotically a straight line, with the same inclination as previously, but shifted upwards by an amount proportional to J . Physically this means that, for a given ‘large’ temperature T_b , the temperature T_a required to run an engine increases with the coupling strength. This can indeed be seen in Figs. 2(b,c). In Fig. 2(d) the upper E -zone exists but is not visible - it has shifted up completely out of the depicted area, since J is so large.

(ii) For $T_b \ll 8J, 2h_b, 2h_a \ll T_a$, the boundary condition, correct to $O(\varepsilon) \sim h_a/T_a \sim J/T_a$, becomes

$$\frac{h_a}{T_a} \left(1 - \frac{2J}{T_a} \right) = \left(1 + \exp\left(\frac{8J - 2h_b}{T_b}\right) \right)^{-1} \quad (\text{B6})$$

Inverting both sides and using the fact that, to same order in ε , $\frac{1}{(1 - \frac{2J}{T_a})} = 1 + \frac{2J}{T_a}$, we obtain

$$T_a = -2J + h_a \left(1 + \exp\left(\frac{8J - 2h_b}{T_b}\right) \right) \quad (\text{B7})$$

When $J > h_a/4$ ($> h_b/4$), Eq. (B7) implies that the minimum temperature T_a necessary for an engine to be possible increases exponentially as $T_b \rightarrow 0$. This remarkable property, which can be clearly seen in Fig 8 above, can be physically understood as follows: recall that $J > h_a/4$ implies that the ground state is the level $-8J$, which does not take part in work exchanges. After the system thermalises with the very cold bath at $T = T_b$, the population of all other levels will be exponentially small, so the same will be true for the amount of work extracted during the dilation stroke. The only way to have an engine in these conditions is to expend an even smaller amount of work in the compression stroke. This is only possible if the populations of levels $\pm 2h$ are exponentially close to each other before the stroke, which in turn requires an exponentially large temperature T_a .

On the other hand, if $J < h_b/4$, the exponential in Eq. (B7) goes quickly to zero for small T_b , and the RHS of this expression becomes $< h_a$. However, this contradicts our starting hypothesis that $T_a \gg h_a$, indicating that there is in fact no physical solution. Indeed, as already noted in the main text (and seen in Figs. 2(a,b)), in this case the E -zone has no boundary at all for small T_b (an engine always becomes possible as $T_b \rightarrow 0$, for any T_a).

b. Boundary of the lower E-zone

For the ‘lower’ E -zone ($T_b > T_a$), we again look for solutions to $f_a = f_b$, but in the limits where (i) T_a is ‘small’ and T_b is ‘large’ or (ii) T_a and T_b are both ‘small’.

(i) For $T_a \ll 8J, 2h_b, 2h_a \ll T_b$ we obtain an equation analogous to Eq. (B6) but with a, b exchanged:

$$\frac{h_b}{T_b} \left(1 - \frac{2J}{T_b} \right) = \left(1 + \exp\left(\frac{8J - 2h_a}{T_a}\right) \right)^{-1} \quad (\text{B8})$$

	W_{cycle}	Q_{hot}	Q_{cold}
Engine	> 0	> 0	< 0
Accelerator	< 0	> 0	< 0
Refrigerator	< 0	< 0	> 0
Heater	< 0	< 0	< 0

TABLE I: The four operational regimes allowed by the First and Second Laws for a thermal machine operating between two thermal reservoirs. Note we use opposite sign conventions for heat and work.

Solving for T_a this time, using the same approximation, we obtain

$$T_a = \frac{8J - 2h_a}{\ln(T_b + 2J - h_b) - \ln(h_b)} \quad (B9)$$

Consistently with Result 1, we see that a solution for an engine in this regime requires $J > h_a/4$.

Note that Eq. (B9) is a (slowly) *decreasing* function of T_b . As discussed in the main text, this implies the very counterintuitive property that, for any fixed T_a , there is a finite value of $T_b > T_a$ above which the cycle ceases to function as an engine.

(ii) For $T_a, T_b \ll 2h_b, 2h_a < 8J$, we use Eq. (B3) for both work functions, obtaining

$$\frac{8J - 2h_a}{T_a} = \frac{8J - 2h_b}{T_b} \quad (B10)$$

or

$$T_a = r_E T_b \quad (B11)$$

with

$$r_E = \frac{4J - h_a}{4J - h_b}. \quad (B12)$$

Note $0 < r_E < 1$ for $J > h_a$.

c. Boundaries of the H-, R- and A -zones

It is worth recalling the conditions defining each zone, which are summarized in Table I above. In terms of energy exchanges, the difference between a *heater* and an *accelerator* is in the sign of Q_{hot} . The boundary between the *H*- and *A*- zones is therefore defined by the condition $Q_{hot} = 0$. Similarly, the difference between a *heater* and a *refrigerator* is in the sign of Q_{cold} , so the boundary between the *H*- and *R*- zones is defined by the condition $Q_{cold} = 0$. For $T_a > T_b$, $Q_{hot} = Q_a$ and $Q_{cold} = Q_b$. From Eqs. (2) and (3), these borders are thus described respectively by the equations

$$8J(p_1^b - p_1^a) = 2h_a(f_a - f_b) \quad (B13)$$

$$8J(p_1^b - p_1^a) = 2h_b(f_a - f_b) \quad (B14)$$

For $2h_j/T_j \sim 8J/T_j \sim \varepsilon \ll 1$, we can use again an iterative method, as with Eq. (B5) above. The solutions to these equations have the linear forms

$$T_a^{AH} = r_{AH} T_b + s_{AH} + O(\varepsilon) \quad (B15)$$

$$T_a^{HR} = r_{HR} T_b + s_{HR} + O(\varepsilon) \quad (B16)$$

where the angular coefficients are respectively

$$r_{AH} = \frac{6J^2 + h_a^2}{6J^2 + h_a h_b} \quad (B17)$$

$$r_{HR} = \frac{6J^2 + h_a h_b}{6J^2 + h_b^2} \quad (B18)$$

while the linear coefficients are respectively

$$s_{AH} = -J \frac{12J^2(r_{AH}^2 - 1) - r_{HR}^2(h_a(2h_a + h_b) + 3h_a^2)}{6J^2 + h_a^2} \quad (B19)$$

$$s_{HR} = -J \frac{12J^2(r_{HR}^2 - 1) + h_a(2h_b + h_a) - 3h_b^2 r_{HR}^2}{6J^2 + h_a h_b} \quad (B20)$$

Note that, for $T_b > T_a$, the roles of Q_a, Q_b invert, so the solutions for the two boundaries are merely swapped (T_a^{AH} would now have the expression in Eq. (B16), and vice-versa). However, since r_{AH} and r_{HR} are both > 1 , these solutions are incompatible with the initial hypothesis ($T_b > T_a$). This implies that, for large $T_a < T_b$, there can be no refrigerator or heater.

Finally, the difference between an *accelerator* and a *refrigerator* is of a different nature. In both cases one bath loses heat while the other one gains; the difference is whether the bath losing heat is the hotter or the colder one. Thus, the boundary between these zones is not marked by a change of sign in either bath's heat exchange, but in the difference of their temperatures. In other words, in this case the boundary is the line

$$T_a^{AR} = T_b, \quad (B21)$$

irrespective of any asymptotic limits. Note this holds both for refrigerators rotating in the 'ordinary' sense (clockwise, $T_a > T_b$), and in the 'counter-rotating' sense (anti-clockwise, $T_b > T_a$).

It is easy to verify that

$$r > r_{AH} > r_{HR} > 1. \quad (B22)$$

This shows that, for large enough T_b , if we start from $T_a = T_b$ and increase T_a , we must obtain in succession a refrigerator, a heater, an accelerator and finally an engine - which is indeed what we observe in Fig. 8. In addition, it also shows that, for large enough T_b , a heater or refrigerator are only possible if $T_a > T_b$ (equivalently, for large enough $T_b > T_a$ only an accelerator or an engine are possible).

d. Strong coupling limit

If J is large compared to h_a, h_b , then it is clear from Eqs. (B12), (B17), (B18) that r_E, r_{AH} and r_{HR} all tend to 1. As a consequence (i) both the H - and R -zones will collapse into an extremely narrow range around the line $T_a = T_b$ (property (vi) in the main text). In addition: (ii) The lower E -zone border will also accompany this line for low T_b , and as a consequence this zone will increase in size. These effects can be seen in Fig. 2(d).

2. Asymptotic Efficiency

Another application of Eqs. (B1)-(B4) is to study the efficiency η in the limit where we have a very cold bath b and a very hot bath a . Suppose

$$T_b \ll 8J < 2h_b < 2h_a \ll T_a. \quad (\text{B23})$$

In this case, we obtain, up to an error of order ε ,

$$W_{cycle} = \frac{2(h_a - h_b) \exp\left[\frac{2h_b - 8J}{T_b}\right]}{1 + \exp\left[\frac{2h_b - 8J}{T_b}\right]} \quad (\text{B24})$$

$$Q_a = \frac{8J + 2h_a \exp\left[\frac{2h_b - 8J}{T_b}\right]}{1 + \exp\left[\frac{2h_b - 8J}{T_b}\right]} - 2J, \quad (\text{B25})$$

so

$$\eta = \frac{2(h_a - h_b) \exp\left[\frac{2h_b - 8J}{T_b}\right]}{6J + 2(h_a - J) \exp\left[\frac{2h_b - 8J}{T_b}\right]} \quad (\text{B26})$$

Choose a fixed value $J = \frac{h_b}{4}(1 - \delta)$ for some $\delta < 1$. Substituting above, we obtain

$$\begin{aligned} \eta &= \frac{2(h_a - h_b) e^{\frac{2h_b \delta}{T_b}}}{\frac{3}{2}h_b(1 - \delta) + (2h_a - \frac{1}{2}h_b(1 - \delta)) e^{\frac{2h_b \delta}{T_b}}} \\ &= \frac{\eta_0 e^{\frac{2h_b \delta}{T_b}}}{\frac{3}{4}r(1 - \delta) + (1 - \frac{1}{4}r(1 - \delta)) e^{\frac{2h_b \delta}{T_b}}} \end{aligned} \quad (\text{B27})$$

It follows that $\eta > \eta_0$ if and only if

$$\frac{3}{4r}(1 - \delta) < \frac{1}{4r}(1 - \delta) e^{\frac{2h_b \delta}{T_b}} \quad (\text{B28})$$

or

$$T_b < \frac{2h_b \delta}{\ln 3} \quad (\text{B29})$$

(for consistency with the hypothesis that $T_b \ll 2h_b$, we see that we must in fact choose $\delta \ll 1$).

In other words, given a sufficiently high coupling strength, there exists a finite threshold for T_b , under which the engine efficiency converges to a higher than

classical value in the limit of high T_a . This is exactly what is seen in Fig. 5(a). For the parameters in that figure ($J = 0.24, h_a = 2, h_b = 1$), it is easy to check that $\delta = 0.04$ and the threshold value is $T_b \sim 0.073$, which matches well with the exact curves. It is also worth noting that, in this limit, W_{cycle} is not negligible; indeed $W_{cycle} \rightarrow 2(h_a - h_b)$ for $T_b \ll 2h_b \delta$.

Another and perhaps more interesting observation is that η in fact *increases further* as T_a is reduced from infinity. To demonstrate this, it is useful to look at $\lim_{T_a \rightarrow \infty} \frac{\partial \eta}{\partial \beta_a}$, where $\beta_a \equiv 1/T_a$ is the inverse temperature. We wish to show that this limit is strictly positive for T_b satisfying Eq. (B29). (Directly calculating $\lim_{T_a \rightarrow \infty} \frac{\partial \eta}{\partial T_a}$ does not give the same information, since in this limit $\frac{\partial \eta}{\partial T_a} = -\frac{1}{T_a^2} \frac{\partial \eta}{\partial \beta_a} \rightarrow 0$)

Going back then to the exact equations for Q_a and W_{cycle} (Eqs. (2)-(7)), replacing $J = \frac{h_b}{4}(1 - \delta)$, and taking the appropriate limits, it is possible to show after some algebra that

$$\lim_{T_a \rightarrow \infty} \frac{\partial \eta}{\partial \beta_a} = \frac{\eta}{W_{cycle}} \left[\eta \left(2h_a^2 + \frac{3}{4}h_b^2(1 - \delta)^2 \right) - 2h_a(h_a - h_b) \right] \quad (\text{B30})$$

Using the asymptotic expression for η in Eq. (B27), we find that the term in square brackets is positive if

$$\exp\left[\frac{2h_b \delta}{T_b}\right] > \frac{3}{1 + \frac{3}{2r}(1 - \delta)}. \quad (\text{B31})$$

In other words:

$$\lim_{T_a \rightarrow \infty} \frac{\partial \eta}{\partial \beta_a} > 0 \iff T_b < \frac{2h_b \delta}{\ln 3 - \ln\left(1 + \frac{3}{2r}(1 - \delta)\right)} \quad (\text{B32})$$

Since this upper bound is strictly larger than the one in Eq. (B29), we arrive at our desired result.

For the parameters in Fig. 5(a), the threshold in Eq. (B32) equals approximately 0.144. It can be seen that η does indeed initially increase with β_a for all values of T_b below this value (including those under the smaller threshold in Eq. (B29)).

Of course, for sufficiently low T_a an engine becomes impossible, so the efficiency must go to zero (at best, this must happen for $T_a < rT_b$). This implies that the efficiency must reach a maximum at some finite T_a , which is what we observe in the figure.

In summary, we have proven

Result 3: Given a sufficiently high coupling strength $J = \frac{h_b}{4}(1 - \delta)$, with $\delta \ll 1$, and a sufficiently low cold bath temperature $T_b \ll 8J$, and taking the limit $T_a \rightarrow \infty$, then the engine efficiency η converges to a value higher than η_0 if and only if T_b is under the threshold given by Eq. (B29). In addition, in these circumstances η increases further as T_a is reduced from infinity, reaching a maximum at some finite T_a .

As discussed in the main text, this is another example of this engine's counter-intuitive behaviours.

[1] F. Binder, L. Correa, C. Gogolin, J. Anders, and G. Adesso (editors), *Thermodynamics in the Quantum Regime*. Fundamental Theories of Physics **195** (Springer, Cham, 2018).

[2] R. Alicki, J. Phys. A: Math. Gen., 12(5):L103 (1979).

[3] R. Kosloff, J. Chem. Phys. **80**, 1625 (1984)

[4] R. Uzdin, A. Levy, and R. Kosloff, Phys. Rev. X **5**, 031044 (2015)

[5] M. O. Scully, K. R. Chapin, K. E. Dorfman, M. B. Kim and A. Svidzinsky, Proc. Nat. Acad. Sci. USA **108**, 15097 (2011).

[6] J. Klatzow, J. N. Becker, P. M. Ledingham, C. Weinzel, K. T. Kaczmarek, D. J. Saunders, J. Nunn, I. A. Walmsley, R. Uzdin and E. Poem, Phys. Rev. Lett. **122**, 110601 (2019).

[7] A.E. Allahverdyan, R. Balian, T.M. Nieuwenhuizen, Europhys. Lett. **67**, 565 (2004).

[8] W. Niedenzu, V. Mukherjee, A. Ghosh, A. G. Kofman and G. Kurizki, Nature Commun. **9**, 165 (2018).

[9] A. Ghosh, W. Niedenzu, V. Mukherjee and G. Kurizki, Chapter 2 in Ref. [1].

[10] J. Roßnagel, O. Abah, F. Schmidt-Kaler, K. Singer and E. Lutz, Phys. Rev. Lett. **112**, 030602 (2014).

[11] C. Elouard, D. Herrera-Martí, B. Huard, and A. Auffèves, Phys. Rev. Lett. **118**, 260603 (2017).

[12] C. Elouard and A. N. Jordan Phys. Rev. Lett. **120**, 260601 (2018).

[13] E. Albayrak, Int. J. Quantum Inf. **11**, 1350021 (2013).

[14] X. L. Huang, H. Xu, X. Y. Niu and Y. D. Fu, Phys. Scr. **88**, 065008 (2013).

[15] J.-Z. He, X. He and J. Zheng, Chin. Phys. B **21** 050303 (2012).

[16] X. He, J.-Z. He and J. Zheng., Physica A **391** 6594 (2012).

[17] X. He and J.-Z. He, Sci. China Phys. Mech. Astron. **55**, 1751 (2012).

[18] T. Zhang, W.-T. Liu, P.-X. Chen, and C.-Z. Li, Phys. Rev. A **75**, 062102 (2007).

[19] G. F. Zhang, Eur. Phys. J. D **49** 123 (2008)

[20] H. Wang, G. Wu and D. Chen, Phys. Scr. **86**, 015001 (2012).

[21] X. L. Huang, Q. Sun, D.Y. Guo and Q. Yu, Physica A **491**, 604 (2018)

[22] G. Thomas and R. S. Johal, Phys. Rev. E **83**, 031135 (2011).

[23] H. T. Quan, Y.-X. Liu, C. P. Sun, and F. Nori, Phys. Rev. E **76**, 031105 (2007).

[24] Tien D. Kieu, Phys. Rev. Lett. **93**, 140403 (2004).

[25] D. V. Schroeder, *An Introduction to Thermal Physics* (Addison-Wesley, Reading, 2000).

[26] M. F. Anka, M.Sc. Thesis, Universidade Federal Fluminense, 2020.

[27] We assume for simplicity units such that the magnetic moment in direction z assumes values $\mu_z = \pm 1$. We also set Boltzmann's constant $k_B = 1$.

[28] These assumptions allow the standard quantum adiabatic theorem to apply. They break down if $J = h/4$ at some point. Thus, for given h_a, h_b , our analysis in this article applies only for $J < h_b/4$ or $J > h_a/4$.

[29] Note this is reversed from the usual *clockwise* representation of an ideal gas heat engine cycle on a $P - V$ or $S - V$ diagram. The physical reason is simple: as h increases adiabatically, so does the gap between the ground and excited states of each spin, which shift equally in opposite directions. This leads to a net loss of energy since the ground state has larger population. However, it takes a higher temperature to maintain the same populations across a wider gap. Thus, as h and T increase, work $W_{b \rightarrow a}$ is extracted from the system, and vice-versa (see Eq. (5)).

[30] In the Supplement [?] we show that, for $T_b < \frac{2h_b(h_b-4J)}{\ln 3}$, $\eta|_{\beta_a \rightarrow 0} > \eta_0$ and $\frac{\partial \eta}{\partial \beta_a}|_{\beta_a \rightarrow 0} > 0$. It can also be shown [22] that η is always upper bounded by $\frac{\eta_0}{1-4J/h_a} < \eta_{Carnot}$.

[31] This conclusion also follows from Eqs. (A6) and (A8).

[32] For example: note that, in the demonstration above, the only place where property (A9) was required was to prove $T_{a1} < T_{b0}$. In the absence of this property, a direct gap would still exist, but it might be entirely within the region where $T_a > T_b$. This would, however, imply an engine existing for $T_a = T_b$, which is forbidden by the Second Law, as discussed in the main text. We therefore conclude that, if a system satisfies properties (A4)-(A8), the Second Law requires it must also satisfy property (A9).